

changes in HIF1 $\alpha$  level itself modifies irradiation response, but both radiosensitization and radioprotection by changes in HIF1 $\alpha$  level have been observed [36]. Further studies, including measurements at longer time points and with administration of other samples, are required to find out if the change in HIF1 $\alpha$  level, with respect to or irrespective of change in tissue oxygen tension, is involved in this particular animal model.

The timing of tumor tissue oxygen tension elevation after artificial oxygen carrier administration differs among previous reports from approximately 4 min to 2 h [9, 28–35]. We do not have a clear answer as to why the increase in tumor tissue oxygen tension was transient in the present study. If the increase in tumor tissue oxygen tension was due to circulating HbV, the effect should have appeared over a longer duration because HbV is known to have a circulating half-life of approximately 48 h [37]. Therefore, we speculated that the increase in tumor tissue oxygen tension may have been affected primarily by extravasated HbV rather than circulating HbV and was hence transient. Tumor vessels are known to be morphologically heterogeneous and has highly permeable sites in comparison to normal vessels. Liposomes ranging in diameter from approximately 100 to 400 nm have been shown to extravasate into the tumor extracellular matrix presumably through these sites [38, 39]. In the present study, human hemoglobin staining revealed the presence of stained material not only within the tumor vasculature but also in the extracellular matrix. We know from previous experiments that hemoglobin is encapsulated within HbV until it is metabolized, which does not occur in this timeframe of 20 min after systemic administration [40]. So we consider that these were extravasated HbV. Lewis lung carcinoma used in this study formed tumors composed primarily of tumor cells and tumor vessels, with very little extracellular matrix. Because of this, the extravasated HbV mostly existed in the vicinity of tumor cells, and hence, may have modulated the tumor response to irradiation. Obviously these results may not be directly applicable to tumors encountered in the clinic, which contain significantly greater amounts of extracellular matrix.

Oxyspot used in this study only measures tissue oxygen tension close to the tissue surface. But since the Lewis lung carcinoma cell line used in this study formed a histologically homogeneous tumor composed primarily from tumor cells and vessels, with little extracellular matrix, we assume that the measurements made in this study sufficiently reflected tissue oxygen tension changes within the whole tumor. To this end, Lewis lung carcinoma line was suitable for this particular study, but its clinical relevance may be limited.

It has been reported that increase in hemoglobin affinity is beneficial for oxygen delivery to normal tis-

sue particularly when oxygen supply is severely compromised [41, 42]. In the present study, there was only a minimal transient increase in tumor tissue oxygen tension after lowP50HbV administration, and benefit was not so apparent. Physiology of oxygen extraction may have been different between different tissues or tumor lines. Blood flow in tumor vessels is known to be highly variable, and regulatory mechanisms may not have functioned as in normal tissue.  $P_{50}$  of 8 Torr in lowP50HbV used in this study may have been too low for significant oxygen release in this particular model. Additionally, in the present study, the increase in tumor tissue oxygen tension may have been due to extravasated rather than circulating HbV, in which case the findings from previous studies which examine materials with low  $P_{50}$  supplying oxygen from within the circulation may not be directly applicable. Further studies are needed to find out if optimization of  $P_{50}$  significantly contributes to oxygenating tumor tissue.

Many types of liposomes are currently being developed to improve selective drug delivery to tumor tissue. HbV used in this study was developed as a transfusion alternative, but it may be possible to increase relative tumor distribution and further optimize HbV's irradiation augmentation effect by modifying its liposomal components as well as its  $P_{50}$ . These improvements may lead to similar or better outcome, with less dosage. The timing of irradiation also needs further study, including the use of fractionation.

#### ACKNOWLEDGMENTS

We thank Mr. Hitoshi Abe, Department of Pathology, School of Medicine, Keio University, for expertise in immunohistochemistry. We also thank Ms. Kyoko Ishiwata, Department of Biochemistry and Integrative Medical Biology, School of Medicine, Keio University, for HIF1 $\alpha$  analysis.

#### REFERENCES

1. Kobayashi K, Tsuchida E, Horinouchi H, eds. *Artificial Oxygen Carrier: Its Front Line*, Keio University International Symposia for Life Sciences and Medicine. Vol. 12, Springer-Verlag, 2005.
2. Chang TM. Hemoglobin based red blood cells substitutes. *Artif Organs* 2004;28:789.
3. Buehler PW, Alayash AI. Toxicities of hemoglobin solutions. in search of in-vitro and in-vivo model systems. *Transfusion* 2004; 44:1516.
4. Djordjevich L, Mayoral J, Miller IF, et al. Cardiorespiratory effects of exchanging transfusions with synthetic erythrocytes in rats. *Crit Care Med* 1987;15:318.
5. Awasthi VD, Garcia D, Klipper R, et al. Neutral and anionic liposome-encapsulated hemoglobin: effect of postinserted poly-(ethylene glycol)-distearoylphosphatidylethanolamine on distribution and circulation kinetics. *J Pharmacol Exp Ther* 2004; 309:241.
6. D'Agnillo F, Alayash AI. Redox cycling of diaspirin cross-linked hemoglobin induces G2/M arrest and apoptosis in cultured endothelial cells. *Blood* 2001;98:3315.
7. Sakai H, Hara H, Yuasa M, et al. Molecular dimensions of

- Hb-based O<sub>2</sub> carriers determine constriction of resistance arteries and hypertension. *Am J Physiol Heart Circ Physiol* 2000;279:H908.
8. Sakai H, Horinouchi H, Yamamoto M, et al. Acute 40 percent exchange-transfusion with hemoglobin-vesicles (HbV) suspended in recombinant human serum albumin solution: Degradation of HbV and erythropoiesis in a rat spleen for 2 weeks. *Transfusion* 2006;46:339.
  9. Sakai H, Horinouchi H, Tomiyama K, et al. Hemoglobin-vesicles as oxygen carriers: Influence on phagocytic activity and histopathological changes in reticuloendothelial system. *Am J Pathol* 2001;159:1079.
  10. Sakai H, Masada Y, Horinouchi H, et al. Physiological capacity of the reticuloendothelial system for the degradation of hemoglobin vesicles (artificial oxygen carriers) after massive intravenous doses by daily repeated infusions for 14 days. *J Pharmacol Exp Ther* 2004;311:874.
  11. Izumi Y, Sakai H, Hamada K, et al. Physiologic responses to exchange transfusion with hemoglobin vesicles as an artificial oxygen carrier in anesthetized rats: Changes in mean arterial pressure and renal cortical tissue oxygen tension. *Crit Care Med* 1996;24:1869.
  12. Izumi Y, Sakai H, Kose T, et al. Evaluation of the capabilities of a hemoglobin vesicle as an artificial oxygen carrier in a rat exchange transfusion model. *ASAIO J* 1997;43:289.
  13. Sakai H, Takeoka S, Wettstein R, et al. Systemic and microvascular responses to the hemorrhagic shock and resuscitation with Hb-vesicles. *Am J Physiol Heart Circ Physiol* 2002;283:H1191.
  14. Sakai H, Masada Y, Horinouchi H, et al. Hemoglobin-vesicles suspended in recombinant human serum albumin for resuscitation from hemorrhagic shock in anesthetized rats. *Crit Care Med* 2004;32:539.
  15. Yoshizu A, Izumi Y, Park S, et al. Hemorrhagic shock resuscitation with an artificial oxygen carrier, hemoglobin vesicle, maintains intestinal perfusion and suppresses the increase in plasma tumor necrosis factor- $\alpha$ . *ASAIO J* 2004;50:458.
  16. Contaldo C, Plock J, Sakai H, et al. New generation of hemoglobin-based oxygen carriers evaluated for oxygenation of critically ischemic hamster flap tissue. *Crit Care Med* 2005;33:806.
  17. Nozue M, Lee I, Manning JM, et al. Oxygenation in tumors by modified hemoglobins. *J Surg Oncol* 1996;62:109.
  18. Takeoka S, Ohgushi T, Terasa K, et al. Layer-controlled hemoglobin vesicles by interaction of hemoglobin with a phospholipid assembly. *Langmuir* 1996;12:1755.
  19. Sakai H, Takeoka S, Park SI, et al. Surface-modification of hemoglobin vesicles with polyethyleneglycol and effects on aggregation, viscosity, and blood flow during 90%-exchange transfusion in anesthetized rats. *Bioconjug Chem* 1997;8:15.
  20. Sakai H, Yusua M, Onuma H, et al. Synthesis and physicochemical characterization of a series of hemoglobin-based oxygen carriers: Objective comparison between cellular and acellular types. *Bioconjug Chem* 2000;11:56.
  21. Maeda N, Imaizumi K, Kon K, et al. A kinetic study on functional impairment of nitric oxide-exposed rat erythrocytes. *Environ Health Perspect* 1987;73:171.
  22. Wilson DF, Cerniglia GJ. Localization of tumors and evaluation of their state of oxygenation by phosphorescence imaging. *Cancer Res* 1992;52:3988.
  23. Ishikawa Y, Kubota T, Otani Y, et al. Dihydropyrimidine dehydrogenase activity and messenger RNA level may be related to the antitumor effect of 5-fluorouracil on human tumor xenografts in nude mice. *Clin Cancer Res* 1999;5:883.
  24. Moeller BJ, Richardson RA, Dewhirst MW. Hypoxia and radiotherapy: Opportunities for improved outcomes in cancer treatment. *Cancer Metastasis Rev* 2007;26:241.
  25. Gray LH, Conger AD, Ebert M, et al. The concentration of oxygen dissolved in tissues at the time of irradiation as a factor in radiotherapy. *Br J Radiol* 1953;26:638.
  26. Deschner EE, Gray LH. Influence of oxygen tension on x-ray-induced chromosomal damage in Ehrlich ascites tumor cells irradiated in vitro and in vivo. *Radiat Res* 1959;11:115.
  27. Lee I, Kim JH, Levitt SH, et al. Increases in tumor response by pentoxifylline alone or in combination with nicotinamide. *Int J Radiat Oncol Biol Phys* 1992;22:425.
  28. Teicher BA, Herman TS, Hopkins RE, et al. Effect of oxygen level on the enhancement of tumor response to radiation by perfluorochemical emulsions or a bovine hemoglobin preparation. *Int J Radiat Oncol Biol Phys* 1991;21:969.
  29. Teicher BA, Holden SA, Ara G, et al. Effect of a bovine hemoglobin preparation (SBHS) on the response of two murine solid tumors to radiation therapy or chemotherapeutic alkylating agents. *Biomater Artif Cells Immob Biotechnol* 1992;20:657.
  30. Teicher BA, Herman TS, Menon K. Enhancement of fractionated radiation therapy by an experimental concentrated perflubron emulsion (Oxygent) in the Lewis lung carcinoma. *Biomater Artif Cells Immob Biotechnol* 1992;20:899.
  31. Teicher BA, Dupuis NP, Robinson MF, et al. Reduced oxygenation in a rat mammary carcinoma post-radiation and reoxygenation with a perflubron emulsion/carbogen breathing. *In Vivo* 1994;8:125.
  32. Teicher BA. An overview on oxygen carriers in cancer therapy. *Artif Cells Blood Substit Immobil Biotechnol* 1995;23:395.
  33. Robinson MF, Dupuis NP, Kusumoto T, et al. Increased tumor oxygenation and radiation sensitivity in two rat tumors by a hemoglobin-based, oxygen-carrying preparation. *Artif Cells Blood Substit Immobil Biotechnol* 1995;23:431.
  34. Linberg R, Conover CD, Shum KL, et al. Increased tissue oxygenation and enhanced radiation sensitivity of solid tumors in rodents following polyethylene glycol conjugated bovine hemoglobin administration. *In Vivo* 1998;12:167.
  35. Kobayashi K, Komatsu T, Iwamaru A, et al. Oxygenation of hypoxic region in solid tumor by administration of human serum albumin incorporating synthetic hemes. *J Biomed Mater Res A* 2003;64:48.
  36. Moeller BJ, Dewhirst MW. HIF-1 and tumour radiosensitivity. *Br J Cancer* 2006;95:1.
  37. Sou K, Klipper R, Goins B, et al. Circulation kinetics and organ distribution of Hb-vesicles developed as a red blood cell substitute. *J Pharmacol Exp Ther* 2005;312:702.
  38. Yuan F, Dellian M, Fukumura D, et al. Vascular permeability in a human tumor xenograft: Molecular size dependence and cutoff size. *Cancer Res* 1995;55:3752.
  39. Yuan F, Leunig M, Huang SK, et al. Microvascular permeability and interstitial penetration of sterically stabilized (stealth) liposomes in a human tumor xenograft. *Cancer Res* 1994;54:3352.
  40. Takeoka S, Teramura Y, Atoji T, et al. Effect of Hb-encapsulation with vesicles on H<sub>2</sub>O<sub>2</sub> reaction and lipid peroxidation. *Bioconjug Chem* 2002;13:1302.
  41. Stein JC, Ellsworth ML. Capillary oxygen transport during severe hypoxia: Role of hemoglobin oxygen affinity. *J Appl Physiol* 1993;75:1601.
  42. Sakai H, Cabrales P, Tsai AG, et al. Oxygen release from low and normal P<sub>50</sub> Hb vesicles in transiently occluded arterioles of the hamster window model. *Am J Physiol Heart Circ Physiol* 2005;288:H2897.

# Hemostatic Efficacy of a Recombinant Thrombin-Coated Polyglycolic Acid Sheet Coupled With Liquid Fibrinogen, Evaluated in a Canine Model of Pulmonary Arterial Hemorrhage

Yotaro Izumi, MD, Masatoshi Gika, MD, Noriko Shinya, DVM, Sumika Miyabashira, BS, Takayuki Imamura, PhD, Chikateru Nozaki, PhD, Masafumi Kawamura, MD, and Koichi Kobayashi, MD

**Background:** In thoracic surgery, although infrequent, we encounter unexpected damage to the pulmonary artery (PA). In the present study, we evaluated the hemostatic efficacy of a newly developed fibrin-based sheet material, thrombin sheet, coupled with liquid fibrinogen (TSF), in an experimental model of PA hemorrhage.

**Methods:** Female beagles ( $n = 8$ ) were used for the study. Left thoracotomy was performed under general anesthesia. PA injury (approximately  $4 \times 2$  mm) was created, and repaired by TSF (TSF group) or TachoComb (TC group). The animals were allowed to survive, and the repaired site was evaluated 4 weeks after the experiment.

**Results:** The number of sheet application and compression procedures required for hemostasis was increased in the TC group compared with in the TSF group (TC vs. TSF,  $4 \pm 1$  vs.  $1 \pm 0.5$ ,  $p = 0.01$ , unpaired  $t$  test). The time required to achieve hemostasis was increased in the TC group compared with in the TSF group (TC vs. TSF,  $7 \pm 3$  vs.  $1 \pm 0.5$  minutes,  $p = 0.01$ , unpaired  $t$  test). The amount of bleeding during the hemostasis procedure was increased in the TC group compared with in the TSF group (TC vs. TSF,  $48 \pm 22$  vs.  $3 \pm 3$  g,  $p = 0.01$ , unpaired  $t$  test). At 4 weeks, rethoracotomy revealed no apparent indication of delayed bleeding, such as intrathoracic hematoma formation or excessive adhe-

sion formation in the vicinity of PA, in either group. Histologically, the vessel lumen was well sustained in both groups, with no apparent stenosis or thrombus formation.

**Conclusion:** The hemostatic efficacy of TSF was superior to TC in this particular experiment. Single application of TSF was sufficient to achieve hemostasis in all but one animal. Compression time of approximately 1 minute was also very short albeit that the bleeding was from the PA and not an artery. These results were presumably because the adhesion was stronger, faster, and the sheet was more pliable in TSF compared with TC.

**Key Words:** Recombinant thrombin sheet, Hemostasis, Pulmonary artery.

*J Trauma.* 2007;63:783-787.

In thoracic surgery, although infrequent, we encounter unexpected damage to the pulmonary artery (PA) resulting in moderate to massive hemorrhage. In most cases, bleeding can be controlled on the spot by manual compression, but compression needs to be released at some point to repair the damage, either to directly suture the vessel, or to sufficiently isolate the vessel, clamp it, and control the bleeding. Significant blood loss can ensue during this period. It will be

possible to reduce this blood loss if a ready-to-use hemostatic material, capable of swift hemostasis becomes available.

Hemostatic materials exploit various mechanisms such as absorbing and concentrating components of blood, increasing the enzymatic activity of clotting factors, or activating platelets.<sup>1-3</sup> Topical hemostatic agents utilizing materials such as cellulose or collagen provide mechanical scaffolds on which thrombus forms, but lack any inherent coagulation potential.<sup>4,5</sup> In this regard, fibrin-based materials can mimic thrombus formation and currently seem to be most effective.<sup>6-11</sup>

We have developed recombinant thrombin,<sup>12,13</sup> which was lyophilized onto a bioabsorbable synthetic nonwoven polyglycolic acid fabric (Neoveil, Gunze K. K., Kyoto, Japan) to yield a new fibrin-based sheet material, thrombin sheet (TS).<sup>14</sup> TS combined with liquid fibrinogen (TSF), is capable of swift hemostasis even when applied inside a blood pool. Fibrinogen solution is dripped onto the sheet immediately before application. Neoveil is loosely fabricated, and the sheet thickness is adjusted to 0.15 mm. This makes TSF quite supple so that it is able to securely conform to the contour of the applied site.

The hemostatic effect of fibrin-based materials in vascular injuries have been evaluated extensively using arterial injury models.<sup>1-3,6,8-11</sup> To our knowledge, control of hemorrhage from the PA has not been adequately assessed.

Submitted for publication February 28, 2006.

Accepted for publication June 26, 2006.

Copyright © 2007 by Lippincott Williams & Wilkins

From the Division of General Thoracic Surgery (Y.I., M.K., K.K.), Department of Surgery, School of Medicine Keio University, Tokyo, Japan; Department of Thoracic Surgery (M.G.), Saitama Medical Center, Saitama Medical School, Saitama, Japan.; Pathology Department (N.S.), Therapeutic Protein Products Research Department (S.M.), and Research Department 1 (T.I., C.N.), The Chemo-Sero-Therapeutic Research Institute (KAKETSUKEN), Kumamoto, Japan.

Address for reprints: Yotaro Izumi, MD, Division of General Thoracic Surgery, Department of Surgery, School of Medicine Keio University, 35 Shinanomachi, Shinjuku-ku, Tokyo 160-8582, Japan; email: yotaro@sc.itc.keio.ac.jp.

DOI: 10.1097/TA.0b013e318151ffdc

Although blood pressure in the artery is much higher in comparison with that of the PA, adequate attachment of the sheet material may be more difficult to achieve in the PA because the vessel wall is more easily deformed by compression. Therefore, materials that control arterial hemorrhage may not necessarily be effective in PA hemorrhage.

In the present study, we evaluated the hemostatic effect of TSF in an experimentally created PA hemorrhage model. The efficacy of TSF was compared in the same model with that of TachoComb (TC) (ZLB Behring Co., Ltd., Bern, Switzerland), a widely used commercially available fibrin-based sheet product. We also measured in vitro fibrin formation in each material as a parameter of hemostatic potential.

## MATERIALS AND METHODS

### Preparation of Thrombin Sheet

Preparation of TS has been described previously.<sup>14</sup> Briefly, mannitol (Nakarai Kagaku, 213-03, Kyoto, Japan), with a final concentration of 0.5% to 1.5%, and 40 mmol/L of calcium chloride were added to a solution containing 0.5% to 2% of glycerol. Recombinant thrombin<sup>12,13</sup> was added to make the final concentration 1,500 U/mL. This solution was dripped at a rate of 0.05 mL/cm<sup>2</sup> and spread evenly using rubber-tipped rods onto a bioabsorptive synthetic nonwoven fabric (3 cm × 3 cm) made of polyglycolic acid, Neoveil (thickness, 0.15 mm). The sheet was frozen at -80°C for 2 hours and dried to fix the recombinant thrombin. The sheet was trimmed to 1.5 cm × 1.5 cm for use in this experiment. The sheet was dipped in 0.2 mL of liquid human fibrinogen (Boheal, Chemo-sero-therapeutic Research Institute, Kumamoto, Japan). The liquid fibrinogen seeped evenly into the sheet within seconds. The sheet was then immediately applied.

### Animal Experiment

Female beagles (Kitayama Labes Co. Ltd., Nagano, Japan) (n = 8) were used for the study. Body weight was measured before induction of anesthesia. Anesthesia was induced by subcutaneous injection of atropine sulfate (0.25 mg per animal), followed 10 minutes after by intramuscular injection of xylazine (1 mg/kg) and ketamine (10 mg/kg). The radial vein was cannulated. Anesthesia was maintained by continuous infusion of 0.1% ketamine in 5% glucose at a rate of approximately 1 mL/min. After injection of suxamethonium (10 mg per animal), the animal was intubated and mechanically ventilated with 40% oxygen. Tidal volume was approximately 200 mL, and respiratory rate was 14 breaths per minute. Empirically, mean systemic arterial blood pressure was maintained at approximately 100 mm Hg during this anesthesia protocol.

The animal was placed in a right lateral position, and left fourth intercostal thoracotomy was performed. The interlobar portion of the left PA was used for the experiment. A 2-mm plastic catheter with an 18-gauge needle tip was gently inserted into the PA, and PA pressure was measured until the values stabilized (for approximately 1 minute). Bleeding dur-

ing this procedure was negligible. Next, the vessel wall adjacent to the needle insertion site was held with fine-toothed forceps, and the vessel wall was resected with fine scissors so as to expand the needle hole proximally. Accounting for the thin and soft PA wall, we preferred this procedure to the use of a punch device. In our preliminary experiment, the laceration thus created was approximately 4 mm × 2 mm. The needle catheter was removed, and free bleeding was visually confirmed for approximately 3 seconds, after which it was controlled by manual compression. Blood in the thoracic cavity was thoroughly suctioned. TSF (TSF group, n = 4) or TC (TC group, n = 4), both 1.5 cm × 1.5 cm in size, was prepared for application. Manual compression was released, and immediately the sheet was applied to cover the laceration. Manual compression was applied over the sheet for 1 minute. If bleeding was not controlled, an additional sheet was applied followed by another minute of manual compression. This was repeated until bleeding was visually controlled. Bleeding during this period was absorbed using gauze, and measured in grams. Hemostasis was confirmed by observation for an additional 10 minutes, and then the chest was closed. Ketoprofen (1 mg/kg) and ampicillin sodium (15 mg/kg) was injected intramuscularly. The animals were allowed to recover and then were returned to their cages. After 4 weeks, the animals underwent rethoracotomy under general anesthesia and the left chest cavity was observed. The interlobar portion of the left PA was carefully inspected for traces of secondary bleeding, for the magnitude of tissue adhesion, and for the presence of residual materials. PA pressure measurement was performed as previously, distal to the site of vessel injury. The animals were killed by pentobarbital overdose, and the left PA was resected together with the left lung. The specimens were fixed in 10% buffered formalin, and embedded in paraffin. Three micrometer paraffin sections were stained with hematoxylin and eosin for histologic examinations.

The School of Medicine Keio University Institutional Animal Care and Use Committee approved all animal studies, which were performed in accordance with the *Guide for the Care and Use of Laboratory Animals* published by the National Academies Press.

Data are shown as mean ± standard deviation. Comparisons were made between groups using unpaired *t* test and within groups using paired *t* test (StatView, SAS Institute Inc., Cary, NC). Significance was assumed at *p* < 0.05.

### In Vitro Measurement of Fibrin Formation

The fibrin clots were prepared for in vitro analysis as follows. In the TC group, a piece of the sheet (0.5 cm × 0.5 cm) was soaked with 50 μL of saline containing 10 U/mL of factor XIII, 50 U/mL of recombinant thrombin, and 25 mmol/L of CaCl<sub>2</sub>, and then incubated for 5, 10, and 30 minutes at 37°C. The reaction was stopped by adding 50 μL of stop solution (4 mol/L urea, 5% sodium dodecyl sulfate [SDS], and 10% 2-mercapto ethanol). Fibrin was dissolved overnight.



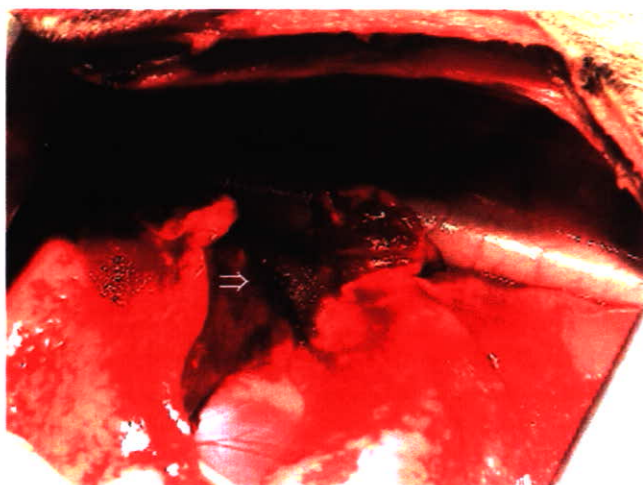


**Fig. 1.** The appearance of thrombin sheet immediately after application. The pulmonary artery laceration can be seen through the applied sheet (arrow).

In the TSF group, 12.5  $\mu$ L of 20 mg/mL fibrinogen containing 25 mmol/L of  $\text{CaCl}_2$  was added to TS (size, 0.5 cm  $\times$  0.5 cm; thrombin, 75 U/cm<sup>2</sup>), and incubated for 5, 10, and 30 minutes at 37°C. The reaction was stopped by adding of 12.5  $\mu$ L stop solution as in the treatment for TC.

SDS-polyacrylamide gel electrophoresis was performed according to the method of Laemmli.<sup>15</sup> About 1  $\mu$ g of fibrinogen was subjected to SDS-polyacrylamide gel electrophoresis on a 7.5% polyacrylamide gel under reducing conditions. The gel was stained with Coomassie brilliant blue R-250.

## RESULTS

All the animals survived. Body weight was comparable between groups before the experiment (TC vs. TSF, 10.0  $\pm$  1.0 vs. 10.4  $\pm$  0.2 kg,  $p = 0.50$ ) and at 4 weeks after the experiment (TC vs. TSF, 11.6  $\pm$  0.9 vs. 11.7  $\pm$  0.6 kg,  $p = 0.1$ ). Within groups, body weight was increased in both groups at 4 weeks after the experiment (TC group  $p = 0.03$ , TSF group  $p = 0.01$ ).

Mean PA pressure was comparable between groups before vessel laceration (TC vs. TSF, 28  $\pm$  5 vs. 27  $\pm$  9 mm Hg,  $p = 0.96$ ) and at 4 weeks after the experiment (TC vs. TSF, 32  $\pm$  3 vs. 30  $\pm$  1 mm Hg,  $p = 0.2$ ). Also, within groups, mean PA pressure was comparable in both groups at 4 weeks after the experiment, compared with values before vessel laceration (TC group  $p = 0.59$ , TSF group  $p = 0.21$ ).

Hemostasis was effectively achieved in both groups after sheet application. In the TSF group, the laceration could be clearly seen through the sheet (Fig. 1, arrow). The number of sheet application and compression procedures required for hemostasis was increased in the TC group compared with in the TSF group (TC vs. TSF, 4  $\pm$  1 vs. 1  $\pm$  0.5,  $p = 0.01$ ). The time required to achieve hemostasis was increased in the TC group compared with in the TSF group (TC vs. TSF, 7  $\pm$  3 vs. 1  $\pm$  0.5 minutes,  $p = 0.01$ ). The amount of bleeding during the hemostasis procedure was increased in the TC group compared with in the TSF group (TC vs. TSF, 48  $\pm$  22 vs. 3  $\pm$  3 g,  $p = 0.01$ ).

At 4 weeks, rethoracotomy revealed no apparent indication in either group of delayed bleeding, such as intrathoracic hematoma formation or excessive adhesion formation in the vicinity of the PA. Macroscopically, adhesion of the lung to the site of sheet application was more apparent in the TC group compared with the TSF group. Residual material was present in both groups, and more prominent in the TC group. Histologically, the vessel lumen was well sustained in both groups, with no apparent stenosis or thrombus formation. However, thickening of the adventitia and the perivascular sheath seemed to be more prominent in the TC group (Fig. 2).

In vitro fibrin formation was more prominent in the TSF group compared with in the TC group. In the TSF group,  $\gamma$ - $\gamma$  cross-linking was formed within 10 minutes, and  $\alpha$ - $\alpha$  polymer was observed. On the other hand, we identified only a trace amount of  $\gamma$ - $\gamma$  cross-linking in TC group (Fig. 3).

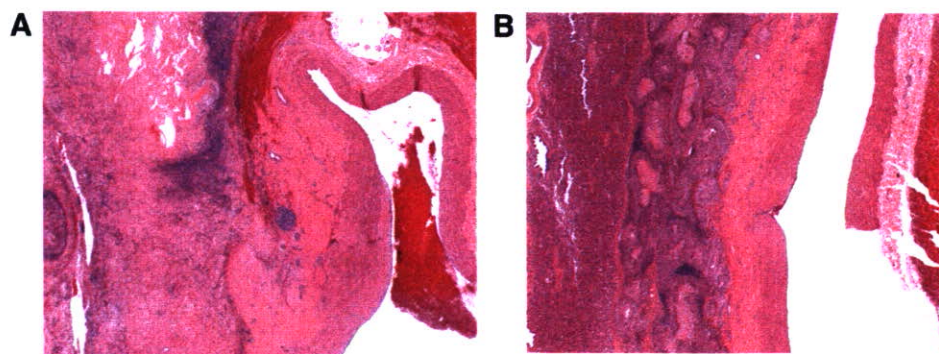


**Fig. 2.** Histologically, the lumen of the repaired vessel was well sustained in both TacoComb (A), and thrombin sheet (B) groups. However, thickening of the adventitia, and the perivascular sheath seemed more prominent in the TacoComb group (A), compared with the thrombin sheet (B) group (Hematoxylin and eosin stain; original magnification,  $\times 2$ ).



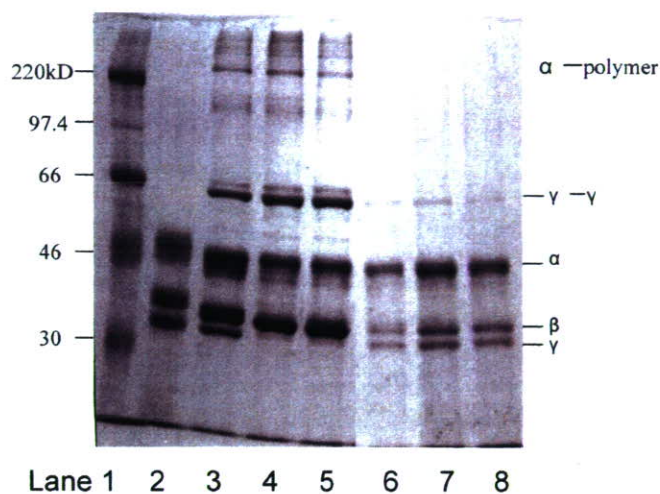


**Fig. 3.** SDS-PAGE of *in vitro* formed fibrin in thrombin sheet plus liquid fibrinogen (TSF group), and TacoComb (TC group). Lane 1, molecular weight marker; lane 2, fibrinogen; lane 3, TSF group reaction for 5 minutes; lane 4, TSF group reaction for 10 minutes; lane 5, TSF group reaction for 30 minutes; lane 6, TC group reaction for 5 minutes; lane 7, TC group reaction for 10 minutes; lane 8, TC group reaction for 30 minutes. *In vitro* fibrin formation was more prominent in the TSF group compared with in the TC group. In the TSF group,  $\gamma$ - $\gamma$  cross-linking was formed within 10 minutes, and  $\alpha$ - $\alpha$  polymer was observed. On the other hand, we identified only a trace amount of  $\gamma$ - $\gamma$  cross linking in TC group.

## DISCUSSION

Fibrin-based sealants have been commercially available in Europe and Japan for many years. Most formulations come as solutions of dissolved thrombin and fibrinogen, which are mixed on application. This form of liquid application is obviously not well suited for hemostasis in vessel injuries where there is significant outflow of blood. Solid material is more suitable because it can withstand the initial outflow of blood, and can be held with pressure after application. To this end, dry fibrin-based hemostatic materials are being developed extensively for potential use, particularly in trauma.<sup>8,9,11</sup> These materials should optimally contain both components, thrombin and fibrinogen, lyophilized onto a sheet material ready for immediate use. Dry materials are also easier to store, particularly for use in combat settings. TC is one such material commercially available in Europe and Japan.<sup>16</sup> Similar dry-sheet type fibrin-based sealants have been extensively evaluated in a variety of hemorrhage models. The results are promising.

Compared with dry materials, TSF is semidry, and may not be ideal for use in trauma settings because liquid fibrinogen needs to be separately prepared. But our attempt to include dry fibrinogen into a sheet material considerably increased the rigidity of the sheet, as is the case with TC. To this end, the TSF is quite supple and conforms considerably better to the contour of the applied site in comparison with how well TC conforms. We considered that this may be

advantageous for bleeding during surgery, particularly from the PA, which is distributed three dimensionally in the thoracic cavity with branching from short segments and is surrounded by lung tissue, which inflates and deflates during ventilation.

In the present study, we investigated the efficacy of fibrin-based sheet type materials in a PA injury model. Hemostasis in vessel injury has been evaluated quite extensively in swine aortic models.<sup>2,8-11</sup> Considering the size of the animals used, approximately 10 kg dogs versus approximately 40 kg pigs, we consider the laceration size in the present study (4 mm  $\times$  2 mm) to be sufficiently large, relative to the laceration size in the widely reported swine model of aortic bleeding (4 mm  $\times$  4 mm). In our preliminary experiment, PA injury could not be controlled by manual compression alone.

Both TSF and TC were capable of adequately controlling PA hemorrhage in this study. Because PA pressure is significantly lower compared with systemic arterial pressure, reduction in blood flow caused by stenosis may more readily ensue compared with the response of arteries of similar caliber. Based on the PA pressure measurements and histologic observations, vessel stenosis or intraluminal thrombosis was not apparent with the use of either material in this study 4 weeks after application, despite the relatively large laceration size. Histologically, thickening of the adventitia and the perivascular sheath was suspected in the TC group, which may in part be because of the increased number of sheet applications.

Overall, the efficacy of TSF was superior to that of TC in this particular experiment. A single application of TSF was sufficient to achieve hemostasis in all but one animal in which the sheet was misplaced, and the vessel laceration was only partially covered on the first application. Compression time of approximately 1 minute was also very short albeit that the bleeding was from the PA and not an artery. These results were observed presumably because the adhesion was stronger, faster, and the sheet was more pliable in TSF compared with in TC.

Fibrinogen is a multidomain protein composed of three polypeptide chains termed  $A\alpha$ ,  $B\beta$ , and  $\gamma$ . Thrombin binds to fibrinogen and cleaves fibrinopeptide A and fibrinopeptide B, and assembles to form fibrin. In the presence of factor XIII and  $Ca^{2+}$ , fibrin undergoes intermolecular covalent cross-linking, which was not as prominent in the TC group compared with in the TSF group. The stronger and faster adhesion may have been at least in part a result of the facilitated formation of fibrin in TSF as shown *in vitro*, although *in vivo* relevance may be less because tissue-derived coagulation factors exist. TSF also allowed for visualization of the laceration through the applied sheet, which was not possible with TC. This enables suturing of the laceration through the TSF for a more definitive hemostasis (data not shown). This property can be considered comparable with what is reported for the American Red Cross fibrin dressing.<sup>8,9</sup> Although we do

not have any experience with this material because of lack of access, the reports indicate that the American Red Cross dressing also achieves superior hemostasis compared with that of TC. Adhesion of TC to the surgical glove during manual compression was another problem. TC had to be gently scraped off the glove with forceps to leave the sheet in place, which was not the case with TSF. Furthermore, after 4 weeks, TSF induced less adhesion compared with TC, suggesting better biocompatibility, although this difference may just be because of the number of applications required. It is true that both materials sufficiently controlled bleeding in this experiment. However, we think that TSF would be much less stressful to use in a setting of unexpected PA bleeding, considering the multiple applications required for TC, as well as the additional blood loss that occurred during this period.

Despite its efficacy, there are certain constraints associated with fibrin-based materials such as availability and cost. It is also true that fibrin-based materials carry a risk of pathogen transmission, although today this is considered to be minimal as a result of improved screening and purification techniques. To alleviate some of these problems, we used recombinant thrombin for TS and development of recombinant fibrinogen is in progress. Ongoing preliminary studies in rabbit aortic injury models also seem to be promising. Studies are necessary to further clarify the hemostatic efficacy of this material in other organ trauma models and in coagulopathic animals.

## ACKNOWLEDGMENTS

We thank Dr. Yuji Nishiwaki, Department of Preventive Medicine and Public Health, for his helpful comments on statistical analysis.

## REFERENCES

- Rothwell SW, Fudge JM, Chen WK, Reid TJ, Krishnamurti C. Addition of a propyl gallate-based procoagulant to a fibrin bandage improves hemostatic performance in a swine arterial bleeding model. *Thromb Res*. 2002;108:335–340.
- Vournakis JN, Demcheva M, Whitson AB, Finkielstein S, Connolly RJ. The RDH bandage: hemostasis and survival in a lethal aortotomy hemorrhage model. *J Surg Res*. 2003;113:1–5.
- Connolly RJ. Application of the poly-*N*-acetyl glucosamine-derived rapid deployment hemostat trauma dressing in severe/lethal Swine hemorrhage trauma models. *J Trauma*. 2004;57:S26–S28.
- Masova L, Rysava J, Krizova P, et al. Hemostyptic effect of oxidized cellulose on blood platelets. *Sb Lek*. 2003;104:231–236.
- Sirlak M, Eryilmaz S, Yazicioglu L, et al. Comparative study of microfibrillar collagen hemostat (Colgel) and oxidized cellulose (Surgicel) in high transfusion-risk cardiac surgery. *J Thorac Cardiovasc Surg*. 2003;126:666–670.
- Jackson MR, Friedman SA, Carter AJ, et al. Hemostatic efficacy of a fibrin sealant-based topical agent in a femoral artery injury model: a randomized, blinded, placebo-controlled study. *J Vasc Surg*. 1997; 26:274–280.
- Jackson MR. New and potential uses of fibrin sealants as an adjunct to surgical hemostasis. *Am J Surg*. 2001;182:36S–39S.
- Sondeen JL, Pusateri AE, Coppes VG, Gaddy CE, Holcomb JB. Comparison of 10 different hemostatic dressings in an aortic injury. *J Trauma*. 2003;54:280–285.
- Pusateri AE, Modrow HE, Harris RA, et al. Advanced hemostatic dressing development program: animal model selection criteria and results of a study of nine hemostatic dressings in a model of severe large venous hemorrhage and hepatic injury in Swine. *J Trauma*. 2003;55:518–526.
- Rothwell SW, Reid TJ, Dorsey J, et al. A salmon thrombin-fibrin bandage controls arterial bleeding in a swine aortotomy model. *J Trauma*. 2005;59:143–149.
- Kheirabadi BS, Acheson EM, Deguzman R, et al. Hemostatic efficacy of two advanced dressings in an aortic hemorrhage model in Swine. *J Trauma*. 2005;59:25–35.
- Soejima K, Mimura N, Yonemura H, Nakatake H, Imamura T, Nozaki C. An efficient refolding method for the preparation of recombinant human prothrombin-2 and characterization of the recombinant-derived alpha-thrombin. *J Biochem (Tokyo)*. 2001; 130:269–277.
- Yonemura H, Imamura T, Soejima K, et al. Preparation of recombinant alpha-thrombin: high-level expression of recombinant human prothrombin-2 and its activation by recombinant ecarin. *J Biochem (Tokyo)*. 2004;135:577–582.
- Uchida T, Shinya N, Kaetsu H, Imamura T, Nozaki C. Thrombin-carrying bioabsorbable synthetic nonwoven fabric, WO 2004/043503.
- Laemmli UK. Cleavage of structural proteins during the assembly of the head of bacteriophage T4. *Nature*. 1970;227:680–685.
- Agus GB, Bono AV, Mira E, et al. Hemostatic efficacy and safety of TachoComb in surgery. Ready to use and rapid hemostatic agent. *Int Surg*. 1996;81:316–319.

## EDITORIAL COMMENT

The authors have demonstrated that a new fibrin-based sheet material that is combined with liquid fibrinogen immediately before use (TSF) provides superior hemostasis when compared with a commercially available fibrin-based sheet material, TachoComb (TC), in a canine model of hemorrhage from an acute pulmonary artery injury. They reference a similar study showing hemostatic superiority of an American Red Cross dry fibrin-based sheet dressing for obtaining hemostasis from acute injury. They, also, reference studies showing excellent hemostasis for systemic arterial hemorrhage, which, of course, occurs at a much higher pressure than that seen from pulmonary artery hemorrhage. Although the authors point out that there are subtle differences in the physics of the injured low-pressure pulmonary artery compared with the high-pressure aortic perforation, the enhanced efficacy of the TSF in this lower arterial pressure system is predictable. Furthermore, the injury described, herein, might be encountered by a thoracic surgeon doing extirpative surgery for intrathoracic tumors but would be rarely encountered in the injured patient who, typically, would have associated lung injury. Thus, the application of this technique to the injured patient is limited.

This reviewer eagerly awaits subsequent reports defining the benefits of this product in the hands of thoracic surgeons.

**Charles E. Lucas, MD**  
Wayne State University  
Detroit, MI

## Syndrome of inappropriate secretion of antidiuretic hormone after chemotherapy with vinorelbine

Hiroaki Kuroda · Masafumi Kawamura · Tai Hato · Kazunori Kamiya ·  
Masahiro Kawakubo · Yotaro Izumi · Masazumi Watanabe ·  
Hirohisa Horinouchi · Koichi Kobayashi

Received: 23 July 2007 / Accepted: 24 October 2007  
© Springer-Verlag 2007

### Abstract

**Purpose** To describe a case of the syndrome of inappropriate secretion of antidiuretic hormone (SIADH) after administration of vinorelbine (VNB) for recurrence of lung cancer.

**Case** A 76-year-old man underwent bronchial arterial infusion (BAI) of VNB for postoperative recurrence of lung cancer. Seven days later, hyponatremia and natriuresis developed. Based on his clinical and laboratory findings, we diagnosed him with SIADH. He improved within a couple of days with fluid restriction only.

**Conclusions** Administration of VNB may potentially cause SIADH. This is the second report of the SIADH caused by VNB. It is important to monitor the serum sodium level and clinical findings after chemotherapy with VNB.

**Keywords** Syndrome of inappropriate secretion of antidiuretic hormone (SIADH) · Vinorelbine (VNB) · Non-small cell lung cancer · Chemotherapy

### Introduction

We present a case of the syndrome of inappropriate secretion of antidiuretic hormone (SIADH) in a 76-year-old man after administration of vinorelbine (VNB). He underwent bronchial arterial infusion (BAI) of VNB for postoperative

recurrence of lung cancer. Seven days later, hyponatremia and natriuresis developed.

Based on his clinical and laboratory findings, we diagnosed him with SIADH. He improved within a couple of days with fluid restriction only. This is the second report of the SIADH caused by VNB therapy for lung carcinoma.

### Case report

A 76-year-old man underwent left upper lobectomy for lung adenocarcinoma (pathological staging T3N1M0, stage IIIA) and 14 months later, chest computed tomography (CT) showed bilateral pulmonary metastases. Five courses of chemotherapy with docetaxel (DOC) 100 mg and gemcitabine (GEM) 1,400 mg resulted in stable disease (SD) and he was begun on modified chemotherapy with vinorelbine (VNB 40 mg). After three courses of VNB, he was admitted to hospital, complaining of left chest pain and cough.

Chest X-ray and CT on admission showed the tumor occluding in the left main bronchus and complete atelectasis of the remaining left lower lobe (Fig. 1a, b).

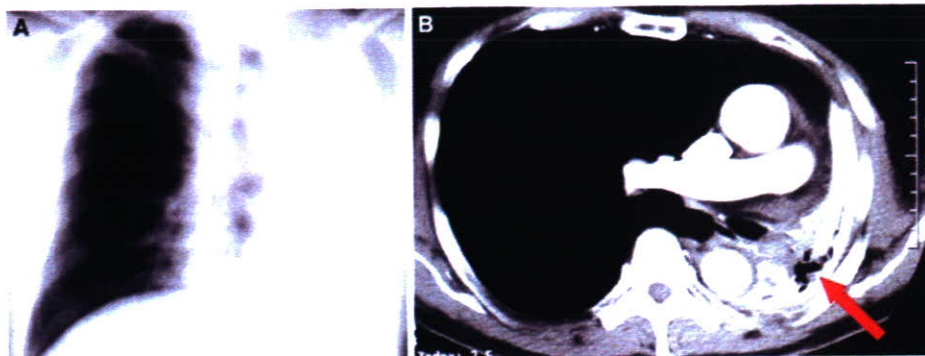
Transbronchial interventions, such as tumor resection, injection of ethanol and YAG laser ablation, were performed repeatedly, after which the chest X-ray showed gradual restoration in his remaining left lobe. Irradiation (total 50 Gy) of the recurrent tumor was performed for 5 weeks and then chemotherapy with VNB 40 mg (BAI 20 mg + intravenous 20 mg) was repeated.

Seven days after administration of 40 mg VNB, he complained of anorexia, nausea and lethargy. His consciousness was clear. His physical and neurogenic examinations were almost intact. His plasma sodium concentration was 113.1 mEq/l, serum osmolality was 242 mOsm/kg lower

H. Kuroda · M. Kawamura (✉) · T. Hato · K. Kamiya ·  
M. Kawakubo · Y. Izumi · M. Watanabe · H. Horinouchi ·  
K. Kobayashi  
Division of General Thoracic Surgery,  
School of Medicine, Keio University,  
35 Shinanomachi, Shinjuku-ku, Tokyo 160-8582, Japan  
e-mail: kawamura@sc.itc.keio.ac.jp



**Fig. 1** **a** Chest X-ray on admission shows complete atelectasis of remaining left lobe. **b** Chest computed tomography scan shows the tumor occluding the left main bronchus (arrow)



than normal limit of 270 mOsm/kg and urine osmolality was 309 mOsm/kg higher than normal limit of 300 mOsm/kg. Urine sodium value was 20.2 mEq/l higher than normal limit of 20 mEq/l. His cortisol concentration value was normal. The plasma arginine vasopressin (AVP) concentration was 0.59 pg/ml, which was within normal limits, as were other parameters. Clinically, there were no symptoms related to adrenal or anterior pituitary dysfunction. The patient was euvolemic and renal function tests were within normal limits. VNB is considered to be strongly associated with SIADH, so he was diagnosed as having SIADH because his clinical features and laboratory data satisfied all standard criteria.

He was treated with water restriction, oral intake plus drip infusion into vein (DIV, total 750 ml/day). Within 2 days, his serum sodium concentration rose gradually and was restored to 130.3 mEq/l (Fig. 2). His mentation and appetite recovered in accordance with the increasing serum sodium concentration without central pontine myelinolysis. There was a possibility of developing SIADH again with a fifth cycle of VNB, so the chemotherapy agent was changed. He has been free of SIADH and has lived with lung cancer for 1 year.

## Discussion

Schwartz et al. first reported SIADH in patients with lung cancer in 1957 [1]. Standard criteria include (1) hyponatremia,

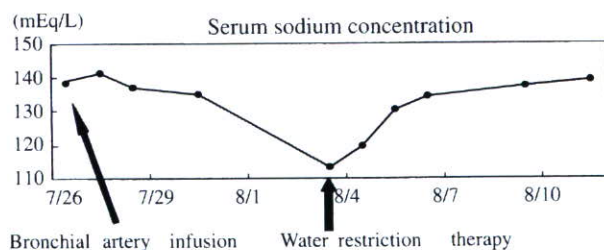


**Fig. 2** Clinical course of serum sodium concentration 7 days after administration of vinorelbine. The patient complained of anorexia, nausea and lethargy and the sodium concentration was 113.1 mEq/l. He was treated with oral water restriction only and 2 days later, the serum sodium concentration was restored to 130.3 mEq/l

(2) plasma hypo-osmolality and urine hyperosmolality, (3) continuous secretion of sodium in urine, (4) normal renal function without hydration, (5) no adrenal gland dysfunction and (6) hyponatremia and hyposmotic pressure that recover with water restriction therapy without change in blood pressure [2]. The present patient fulfilled these criteria.

Various causes of SIADH have been reported, such as disorders of the cerebral nervous system, malignant tumors, diseases of the thoracic cavity, medicinal side-effects and idiopathic [3]. Approximately 75% of tumor-associated cases of SIADH are related to small-cell lung cancer (SCLC) [4]. The occurrence of SIADH with non-small-cell carcinoma (NSCLC) has been only rarely reported [5]. It has been reported that SIADH is caused by the tumor invading the vagus nerve or releasing ADH-like product. In the present study, imaging showed no evidence of invasion of the vagus nerve and we identified that the serum level of AVP was normal. We do not consider that its upregulation or secretion of ADH-like material occurred because the patient never experienced other electrolytic abnormalities and his serum sodium concentration was restored rapidly by water restriction therapy alone. There was no evidence of a relationship between progression of lung carcinoma and the onset of SIADH in this case.

Another possibility is that when the extension receptors of the left atrium detect hyperthoracic pressure and abnormal hemodynamics, they decrease the suppressor signal level and induce continuous release of ADH from the posterior lobe of the pituitary. But in the present case, bronchoscopic interventions were performed to target the local recurrence and restore his remaining left lobe. Syndrome of inappropriate secretion of antidiuretic hormone developed after 5 weeks of irradiation therapy following these interventional procedures. Even if there was a change in the respiratory circulation with release of the atelectasis, it is unlikely because of the time delay.

Enhancing release of AVP, potentiating the renal action of AVP and unknown mechanisms are reported as the main causes of SIADH by drugs [3]. Syndrome of inappropriate secretion of antidiuretic hormone associated with vinca

alkaloids, especially vincristine (VCR) and vinblastine (VBL), has been reported [6–8]. Garrett and Simpson first reported that SIADH occurred after a single treatment of VNB for breast cancer [9]. In addition, they reported that there was a slight structural difference between VNB and other vinca alkaloids, however, the precise mechanism is unclear and they may possess common neural or renal adverse effect profiles. In the present case, we firmly concluded that SIADH was induced by chemotherapy with VNB because concomitant medication was steroids only. In addition, SIADH occurred after four courses and not with earlier exposures of VNB. Although we think that repeated administration or retention of VNB may have been associated with SIADH, the precise mechanism of this SIADH was unclear.

In the report by Garrett and Simpson, SIADH from VNB did not respond to fluid restriction and patient had to be given 3% NS. But in our case, patient recovered with fluid restriction only. This difference with these two mechanisms was unclear. Furthermore, they also reported that prophylactic use of demeclocycline, which interacts with ADH at the renal collecting duct, might usefully prevent recurrence of SIADH associated with continuous treatment with VNB [9]. Stuart and Cuaso reported that SIADH was prevented by rigorous water restriction [10]. For our patients, we choose an alternative because of the high possibility of SIADH caused by VNB. If chemotherapy with VNB results in complete response or partial response, we would choose to readminister VNB with restriction of water, or use demeclocycline and monitor the sodium concentration.

We consider that VNB should be regarded as very likely to cause SIADH, but as this is only the second report of SIADH associated with use of VNB alone, it is a rare occurrence.

## Conclusion

It is known that lung cancer can give rise to SIADH as a paraneoplastic syndrome and there are some anticancer agents that can potentially cause SIADH. It is important to monitor the serum sodium level and clinical findings after chemotherapy for lung cancer.

## References

1. Schwartz WB, Bennet W, Curelop S, et al (1957) A syndrome of renal sodium loss and hyponatremia probably resulting from inappropriate secretion of antidiuretic hormone. *Am J Med* 23:529–542
2. Barter FC, Schwartz WB (1967) The syndrome of inappropriate secretion of antidiuretic hormone. *Am J Med* 42:790–806
3. Reynolds RM, Seckl JR (2005) Hyponatraemia for the clinical endocrinologist. *Clin Endocrinol* 63:366–374
4. Tho LM, Ferry DR (2005) Is the paraneoplastic syndrome of inappropriate antidiuretic hormone secretion in lung cancer always attributable to small cell variety? *Postgrad Med J* 81:e17
5. Sorensen JB, Anderson, Hansen HH (1995) Syndrome of inappropriate of antidiuretic hormone (SIADH) in malignant disease. *J Intern Med* 238:97–110
6. Fraschini G, Recchia F, Holmes FA (1987) Syndrome of inappropriate antidiuretic hormone secretion associated with hepatic arterial infarction of vinblastine in three patients with breast cancer. *Tumor* 73:513–516
7. Robertson GL, Bhoopalam N, et al (1973) Vincristine neurotoxicity and abnormal secretion of antidiuretic hormone. *Arch Intern Med* 132:717–720
8. Kawamae K, Ganaha F, et al (1993) A case of inappropriate secretion of antidiuretic hormone (SIADH) and renal dysfunction by cisplatin. *ICU CCU* 17:587–592
9. Garrett CA, Simpson TA Jr (1998) Syndrome of inappropriate antidiuretic hormone associated with vinorelbine therapy. *Ann Pharmacother* 32:1306–1309
10. Stuart MJ, Cuaso C, et al (1975) Syndrome of recurrent increased secretion of hormone following multiple doses of vincristine. *Blood* 45:315–320

# Cross-linked poly (gamma-glutamic acid) attenuates peritoneal adhesion in a rat model

Yotaro Izumi, MD, PhD,<sup>a</sup> Michiko Yamamoto, BS,<sup>b</sup> Masafumi Kawamura, MD, PhD,<sup>a</sup> Takeshi Adachi, MD, PhD,<sup>b</sup> and Koichi Kobayashi, MD, PhD,<sup>a</sup> Tokyo, Japan

**Background.** Poly (gamma-glutamic acid) (PGA) is a naturally occurring biodegradable polymer produced by *Bacillus subtilis*. PGA is crosslinked by gamma-irradiation to yield crosslinked PGA (XL). XL absorbs large amounts of fluid and forms a biodegradable viscous hydrogel. In the present study, we evaluated the anti-adhesive effect of XL in a rat abdominal wall defect and cecal abrasion model.

**Methods.** Abdominal wall resection and cecal abrasion were carried out in rats (abrasion-no-treatment group, n = 12). In the treatment groups, the following materials were applied: PGA (n = 12), XL (n = 16), hyaluronic acid (HA) (n = 12), Seprafilm (n = 12), and Interceed (n = 10). A week later, adhesion formation was evaluated.

**Results.** Firm adhesions were seen in the abrasion-no-treatment group. XL reduced adhesion formation significantly compared with abrasion-no-treatment, HA, Seprafilm, and Interceed groups. Although not statistically significant, the magnitude of adhesion formation was decreased in the XL group in comparison to the PGA group.

**Conclusions.** We suggest that the anti-adhesive effect of XL was superior to other materials in this rat model. XL application may have attenuated tissue adhesion by forming a viscous hydrogel over the injured surfaces. (*Surgery* 2007;141:678-81.)

From the Department of Surgery, Division of General Thoracic Surgery,<sup>a</sup> and Department of Biochemistry and Integrative Medical Biology,<sup>b</sup> School of Medicine, Keio University, Tokyo, Japan

THE CONSEQUENCES OF ADHESIONS after abdominal operation include small-bowel obstruction, infertility, chronic abdominal pain, and difficulty of a second operation. As longevity is increased, more patients are likely to undergo multiple operative procedures during their lifetime. With the advent of minimally invasive video-assisted operation, the frequency and magnitude of postoperative adhesion formation has decreased dramatically in all fields of operation. Adhesion formation, however, occurs to some extent even in video-assisted operation, and there are still many instances where open operation is required. The search for an effective anti-adhesive agent has been ongoing for

decades. Although some agents have shown promise in preclinical and clinical studies, their efficacy currently is by no means satisfactory.

Poly (gamma-glutamic acid) (PGA) is a naturally occurring, biodegradable polymer produced by a strain of *Bacillus subtilis*.<sup>1</sup> PGA can be crosslinked by gamma-irradiation to yield crosslinked PGA (XL). In the presence of fluid, XL forms a biodegradable viscous hydrogel capable of holding water approximately 1,400 times its dry volume.<sup>2</sup> There are many ways to crosslink polymers such as PGA to create hydrogels with high water absorption. Among these, irradiation is most convenient, because it uses no chemical agents that require subsequent removal, and it often expedites the need for additional sterilization. Research into the application of XL for cosmetics, purification of sewage, drug delivery systems, and reforestation is in progress currently. Based on its ability to absorb fluid and form a viscous hydrogel, we hypothesized that XL may be effective as an anti-adhesive agent. In the present study, we evaluated the anti-adhesive effect of XL in a rat abdominal wall defect and cecal abrasion model.

Accepted for publication December 14, 2006.

Reprint requests: Yotaro Izumi, Department of Surgery, Division of General Thoracic Surgery, School of Medicine Keio University, 35 Shinanomachi, Shinjuku-ku, Tokyo 160-8582, Japan. E-mail: yotaro@sc.itc.keio.ac.jp.

0039-6060/\$ - see front matter

© 2007 Mosby, Inc. All rights reserved.

doi:10.1016/j.surg.2006.12.010



## MATERIALS AND METHODS

**Animal experiment.** Male Donryu rats, 5 to 7 weeks old, weighing 150 to 200 g (Saitama-jikkenn, Saitama, Japan) were used for this study. The animals were housed 3 per cage in a temperature-controlled, 12-hour light/dark-cycled room with free access to food and water. The rats were anesthetized with an intramuscular injection of a cocktail of 90 mg ketamine hydrochloride (Parke-Davis, Morris Plains, NJ) and 9 mg xylazine (Fermentia, Kansas City, MO) per kg body weight. Operative procedures were carried out in a semi-sterile environment under a heating lamp. Abdominal wall resection and cecal abrasion was carried out as reported previously.<sup>3</sup> In brief, the ventral hair was clipped with an electric shaver, and the abdominal skin was painted with 70% alcohol. A 5-cm midline abdominal incision was made. In all the rats used, the cecum was located to the left of midline. The left abdominal wall covering the cecum was retracted. A 1 × 2 cm segment of parietal peritoneum directly anterior to the cecum was excised sharply from the abdominal wall including a layer of underlying muscle. The defect was then abraded by rubbing with a dry gauze. The cecum was also abraded by rubbing with dry gauze so that a homogenous surface of petechial hemorrhage was created over a 1 × 2 cm surface. Both the abdominal wall defect and the abraded cecum were dried in hot air with a hair dryer for 20 seconds, and then exposed to room air for 10 minutes. The rest of the abdominal contents were protected from drying by placement of moistened gauze. The abraded areas were then placed in contact, and the midline incision was closed (abrasion-no-treatment group, n = 12). The animals were allowed to recover from anesthesia, and were returned to their cages.

In the treatment groups, the following materials were placed between the abraded areas at closure. PGA (BioPGA, Meiji Seika Kaisha Ltd, Tokyo, Japan), (PGA group, n = 12), XL (BioPGA-XL, Meiji Seika Kaisha Ltd) (XL group, n = 16), hyaluronic acid (HA group, n = 12) (molecular weight  $2 \times 10^5$ ; Meiji Seika Kaisha Ltd), Seprafilm (Seprafilm group, n = 12) (Genzyme Corp. Cambridge, MA), and Interceed (Interceed group, n = 10) (Ethicon Inc. Somerville, NJ). BioPGA and BioPGA-XL are powders. In the PGA and XL groups, BioPGA or BioPGA-XL was sprinkled to cover the abraded area. In the HA group, HA was applied as a 0.4% solution in phosphate buffered saline as reported previously.<sup>4</sup> Two milliliters of the solution was applied over the abraded area and allowed to spread in the abdominal cavity. Se-

prafilm and Interceed are sheets. In the Seprafilm and Interceed groups, the sheets were trimmed and applied so that the entire abraded areas were covered completely. One surgeon (Y.I.) carried out all the operations but was blinded to the randomization while carrying out the abrasions.

Seven days later, the rats were anesthetized, and a relaparotomy was carried out through a right paramedian incision to avoid damaging the site of adhesions. Adhesions were scored by a adhesion severity scoring system reported previously<sup>5</sup>:

- 0 = no adhesions;
- 1 = loose filmy adhesions that can be separated by blunt dissection;
- 2 = adhesions requiring less than 50% of sharp dissection for separation;
- 3 = adhesions requiring greater than 50% of sharp dissection for separation;
- 4 = serosal injury;
- 5 = full-thickness injury.

Scoring was done by M.K. who was blinded to the group assignment. Scores were averaged within groups.

Body weight of the animals were measured before operation and 7 days after before scoring the adhesion. For comparison, body weight also was measured in animals receiving no intervention (control group, n = 6), and in animals receiving anesthesia and laparotomy without abrasion (laparotomy-only group, n = 6).

All animal studies were approved by the School of Medicine Keio University Institutional Animal Care and Use Committee and were carried out in accordance with the "Guide for the Care and Use of Laboratory Animals" published by the National Institute of Health.

Data are presented as mean  $\pm$  standard deviation. Adhesion scores were compared between groups using Kruskal-Wallis Dunn's test (StatMate III, ATMS, Ltd, Tokyo, Japan). Changes in body weight were compared between groups using ANOVA Bonferroni's test (StatView, SAS Institute, Cary, NC). Significance was assumed at *P* less than .05.

## RESULTS

**Animal experiment.** The distribution of adhesion scores is shown in the Table. With the exception of 1 animal, adhesions were absent in the XL group. The average adhesion score was less in XL ( $0.1 \pm 0.3$ ) compared with the other groups of abrasion-no-treatment ( $3.4 \pm 1.1$ ), HA ( $3.0 \pm 0.9$ ), Seprafilm ( $1.8 \pm 0.6$ ), or Interceed ( $2.4 \pm 0.8$ ). The average adhesion score did not differ between

**Table.** Distribution of adhesion scores in each group are shown

Group adhesion score	Abrasion- no- treatment	PGA†	XL*	HA	Seprafilm	Interceed
0	0	9	15	0	0	0
1	1	5	1	0	3	1
2	0	2	0	5	8	5
3	6	0	0	3	1	3
4	3	0	0	4	0	1
5	2	0	0	0	0	0

HA, hyaluronic acid; PGA, poly (gamma-glutamic acid); XL, cross-linked poly (gamma-glutamic acid).

\*Differs from all other groups except PGA ( $P < .05$ ).

†Differs from abrasion-no-treatment, HA, and Interceed ( $P < .05$ ).

the XL and PGA groups ( $0.6 \pm 0.7$ ). The average adhesion score was less in PGA group compared with abrasion-no-treatment, HA, or Interceed groups, but not in comparison to the Seprafilm group. There were no differences between the abrasion-no-treatment, HA, Seprafilm, or Interceed groups.

No apparent changes in behavior were seen in any of the animals. The percent changes in body weight in the abrasion-no-treatment, PGA, XL, HA, Seprafilm, and Interceed groups were  $93 \pm 3$ ,  $104 \pm 7$ ,  $105 \pm 6$ ,  $93 \pm 4$ ,  $97 \pm 6$ , and  $97 \pm 7$ , respectively. Body weight remained greater in the Seprafilm, Interceed, PGA, and XL group compared with abrasion-no-treatment, and HA groups, but only PGA, and XL groups reached statistical significance. In the control and laparotomy-only groups, the percent increase in body weight during 7 days were  $138 \pm 3$  and  $119 \pm 3$ , respectively. Increases in weight were greater in the control group compared with the laparotomy-only group and in the laparotomy-only group compared with any of the animals that underwent abrasion ( $P < .05$  each).

## DISCUSSION

Mechanical separation of injured surfaces is a strategy for preventing the formation of tissue adhesion. Ideally, the material should be easily applicable, biodegradable without systemic effects, and can be applied repetitively if multiple operations are required. Materials of this kind come in various forms including liquid, powder, and sheet preparations. We evaluated the formation of adhesions in this rat model 7 days after operation based on a number of studies that indicate that adhesions become established within 7 days of tissue injury<sup>3</sup> and because in a rat model, adhesions presenting at 1

week were persistent at 6 months.<sup>6</sup> The extent of tissue injury in this experiment was probably greater than what we encounter commonly in clinical practice, but adhesions of this magnitude may be present in patients who have undergone multiple operations. The increase in body weight during the 7-day observation period was suppressed in these groups receiving abrasion compared with only-laparotomy. This suppression in weight gain may have been attenuated by the application of the anti-adhesive materials of PGA and XL. The results also showed that weight suppression was not attributable to any of the materials applied.

In the present study, the efficacy of HA was not clear, consistent with previous reports indicating its efficacy only when applied before abrasion is created.<sup>4</sup> Lubricating agents such as HA have shown some effect when used before injury, but this is not always possible in clinical practice. The sheet materials of Seprafilm and Interceed are available commercially. Although the average adhesion scores did not differ from the abrasion-no-treatment group, their efficacy in this study was comparable to previous preclinical studies using these materials in various laparotomy models, notwithstanding that the models differ slightly from study to study.<sup>5,7</sup> Both these agents decreased the severity of adhesion formation, but sharp dissection was required to some extent in most animals. Although our study groups were relatively small, the anti-adhesive effect of XL seems to be superior to other materials in this particular model. Although the difference in the average adhesion score between XL and PGA did not differ, adhesions were absent in the XL group with the exception of 1 animal; thus, we believe that this material deserves further investigation. The efficacy of anti-adhesive agents is reported to be related, at least in part, to the agents' viscosity, its ability to coat the wounded surface, and the residence time at the site of injury.<sup>3</sup> We know that XL forms a viscous hydrogel, and this hydrogel may have coated effectively the wounded surface for a sufficient period of time. Further studies are necessary to elucidate the exact mechanisms involved.

One may question the dose-equivalency between the different forms of the materials used in this study. Although it is not possible to compare explicitly liquid, powder, and sheet, in the present study, materials other than PGA and XL were used according to previous reports. As for PGA and XL, we used the minimum amount required to cover sufficiently the abraded area. Further dose-efficacy studies along with studies on potential side effects are necessary to determine the most appropriate

dose. Each material has advantages and drawbacks. Liquid materials such as HA disperse in the abdominal cavity. Some investigators claim this property to be beneficial, because it interferes with all potential adhesion formation. Prevention of adhesions remote from the site of application may not, however, always be advantageous. Adhesions may represent the process of healing and thereby function to prevent or ameliorate postoperative bleeding or dehiscence of gastrointestinal anastomoses. The use of drainage tubes after operation may evacuate extravasated secretions or exudate in the abdominal cavity, and at the same time, the anti-adhesive material may interfere with this drainage. To this end, sheet materials, such as Seprafilm and Interceed, provide localized anti-adhesive effect, but materials in the forms of liquid or powder may be more easily applicable from the ports in video-assisted operation. Because XL forms a hydrogel by absorbing surrounding fluid, it eventually disperses in the abdominal cavity with time. This property may be overcome by embedding the powder in a sheet material to provide better localization. It may also be possible to incorporate factors that regulate adhesion formation within the XL hydrogel. Further studies are necessary to evaluate the anti-adhesive effect of XL, including studies in relaparotomy models, as well as other models of adhesion. Regarding its safety, studies in experimental models including intraperitoneal gastrointestinal anastomoses are necessary because this

material may interfere with wound healing of anastomoses. We assume that the XL in the abdominal cavity is degraded by hydrolysis and absorbed, but long-term observations are necessary to further define its metabolism.

We thank Dr. Yuji Nishiwaki, Department of Preventive Medicine and Public Health, for his comments on the statistical analyses.

#### REFERENCES

1. Shih IL, Van YT. The production of poly-(gamma-glutamic acid) from microorganisms and its various applications. *Bioresour Technol* 2001;79:207-25.
2. Choi HJ, Kunioka M. Preparation conditions and swelling equilibria of hydrogel prepared by gamma-irradiation from microbial poly (gamma-glutamic acid). *Radiat Phys Chem* 1995;46:175-9.
3. Harris ES, Morgan RF, Rodeheaver GT. Analysis of the kinetics of peritoneal adhesion formation in the rat and evaluation of potential anti-adhesive agents. *Surgery* 1995;117:663-9.
4. Yaacobi Y, Israel AA, Goldberg EP. HA Prevention of postoperative abdominal adhesions by tissue precoating with polymer solutions. *J Surg Res* 1993;55:422-6.
5. Oncel M, Remzi FH, Senagore AJ, Connor JT, Fazio VW. Comparison of a novel liquid (Adcon-P) and a sodium hyaluronate and carboxymethylcellulose membrane (Seprafilm) in postsurgical adhesion formation in a murine model. *Dis Colon Rectum* 2003;46:187-91.
6. Ryan GB, Grobety J, Majno G. Postoperative peritoneal adhesions. A study of the mechanisms. *Am J Pathol* 1971; 65:117-48.
7. Ryan CK, Sax HC. Evaluation of a carboxymethylcellulose sponge for prevention of postoperative adhesions. *Am J Surg* 1995;169:154-9.



# Hyperthermia-enhanced tumor accumulation and antitumor efficacy of a doxorubicin-conjugate with a novel macromolecular carrier system in mice with non-small cell lung cancer

TAKAHIKO OYAMA<sup>1</sup>, MASAFUMI KAWAMURA<sup>1</sup>, TOMOHIRO ABIKO<sup>1</sup>, YOTARO IZUMI<sup>1</sup>,  
MASAZUMI WATANABE<sup>1</sup>, EIJI KUMAZAWA<sup>2</sup>, HIROSHI KUGA<sup>2</sup>,  
YOSHINOBU SHIOSE<sup>2</sup> and KOICHI KOBAYASHI<sup>1</sup>

<sup>1</sup>Division of General Thoracic Surgery, Department of Surgery, School of Medicine, Keio University, 35 Shinanomachi, Shinjuku-ku, Tokyo 160-8582; <sup>2</sup>New Product Research Laboratories III, Daiichi Pharmaceutical Co., Ltd., 16-13, Kita-Kasai 1, Edogawa-ku, Tokyo 134-8630, Japan

Received October 12, 2006; Accepted November 16, 2006

**Abstract.** A novel drug delivery system (DDS) compound was formed by binding doxorubicin hydrochloride (DXR) to the macromolecular carrier carboxymethyl dextran polyalcohol (CM-Dex-PA) via the peptidyl spacer (GGFG: Gly-Gly-Phe-Gly). Its use in a murine tumor model confirmed that the DDS (CM-Dex-PA-GGFG-DXR) was retained in the blood and distributed in tumor tissue. The combined use of hyperthermia (HT: 41-42°C for 40 min) and DXR-conjugate (5, 10 or 20 mg/kg i.v.) on tumor accumulation and efficacy was investigated in a murine model of non-small cell lung cancer. Tumor size was measured and the tumor inhibition rate (IR) was calculated. The mean tumor concentration of conjugated DXR in the DXR-conjugate group was 9.40 µg/g compared with 19.04 µg/g in the DXR-conjugate + HT group (p=0.0008). The antitumor efficacy of the DXR-conjugate was significantly enhanced in the groups receiving the combination therapy (p=0.0039, p=0.0250). Significant differences were found between the groups given DXR and those given DXR-conjugate (p=0.0492, p=0.0104). The results demonstrate that the antitumor efficacy of DXR-conjugate is significantly superior to that of DXR alone and the combined use of DXR-conjugate and HT increases the drug's concentration in the tumor, with significant enhancement of antitumor efficacy.

## Introduction

Conventional anticancer drugs have poor selective cytotoxicity, and severe side effects are a dose-limiting factor (1). Therefore, selective targeting of tumors by anticancer drugs is needed. Solid tumors generally possess some pathophysiological characteristics that lead to what is known as the 'EPR' effect (enhances permeability and retention) (2-6): a) hyper-vascularity; b) incomplete vascular architecture; c) secretion of vascular permeability factors that stimulate extravasation within the cancer; and d) little drainage of macromolecules and particles, which results in their long-term retention in the tumor.

The doxorubicin hydrochloride (DXR)-conjugate [macromolecular carrier peptidyl spacer (GGFG)-DXR, carboxymethyl dextran polyalcohol (CM-Dex-PA)-GGFG-DXR] synthesized in the present study is retained in high concentration in the blood for a long time because of the nature of the CM-Dex-PA carrier, which enables passive tumor targeting based on the EPR effect (7-9). CM-Dex-PA has high water-solubility, thus enabling its conjugate to also be water-soluble. The main chain, dextran polyalcohol (Dex-PA), has structural flexibility and a similarity to polyethylene glycol (PEG) so it is not recognized as a foreign body by the reticuloendothelial system. Because its mean molecular weight is approximately 300 kilodaltons (kDa), it does not pass through the glomerular filter. Accumulation of DXR-conjugate in tumor tissue is proportional to the tumor blood flow and vascular permeability. The macromolecule is incorporated into tumor cells by endocytosis and DXR is released from the peptidyl spacer (GGFG: Gly-Gly-Phe-Gly) by lysosomal enzymes (i.e., cathepsins). After the DXR is released, CM-Dex-PA is slowly depolymerized in the lysosomal acidic environment and excreted (10,11) (Fig. 1).

We reviewed the literature for a new drug delivery system (DDS) compound and focused our attention on hyperthermia (HT), which is a recognized modality in interdisciplinary oncotherapy. HT alters the local tumor environment (12,13) and has a lethal effect on cancer cells, even when it is used

---

*Correspondence to:* Dr T. Oyama, Division of General Thoracic Surgery, Department of Surgery, School of Medicine, Keio University, 35 Shinanomachi, Shinjuku-ku, Tokyo 160-8582, Japan  
E-mail: t.oyama@ashikaga.jrc.or.jp

**Key words:** drug delivery system, doxorubicin hydrochloride-conjugate, macromolecular carrier, non-small cell lung cancer, hyperthermia

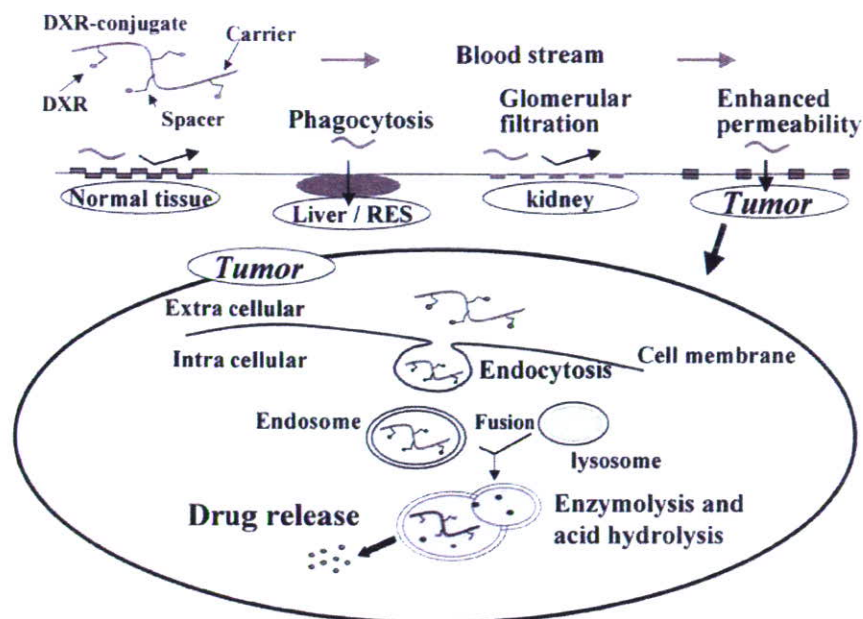


Figure 1. Schematic of passive tumor-targeting based on the EPR (enhanced permeability and retention) effect and drug-release mechanism of the doxorubicin (DXR)-conjugate.

alone (14). Tumor blood flow (15,16) and the permeability of tumor vessels (17-20) are increased at temperatures of 41-43°C. Efficacy is enhanced by combined use with irradiation or anticancer drugs, so the present study was designed to investigate both the usefulness of DXR-conjugate in comparison with DXR alone and the usefulness of combining HT with DXR-conjugate in mice with non-small cell lung cancer (NSCLC).

## Materials and methods

**Animals and tumor model.** Male 5-week-old BALB c-nu/nu nude mice (CLEA Japan Inc.) were used and the tumor model was created by subcutaneously injecting NSCLC strain LU99 cells (large cell carcinoma;  $1 \times 10^5$  cells). The long (L) and short (W) diameters of the tumor were measured with calipers and the weight was estimated as:  $V = (L \cdot W \cdot W)/2$  (mg). The experiment was started when the estimated weight of the implanted tumors reached 200-400 mg (10-16 days after implantation).

**DXR-conjugate.** The DXR-conjugate (CM-Dex-PA-GGFG-DXR; Daiichi Pharmaceutical Co.) had 0.4% carboxymethylation, whereas the DXR content was 6.8% (Fig. 2).

**Hyperthermia.** Hyperthermia was achieved with a Thermotoron RF IV, a radiofrequency-type warmer apparatus used for animals and now widely used in the clinical setting (frequency, 8 MHz; maximum output, 200 W; Yamamoto Vinita Co., Ltd.). Radiofrequency waves at frequencies <100 MHz will warm deep tissue. The mice were anesthetized with pentobarbital (40 mg/kg i.p.) for immobilization during the 40-min HT period. The subcutaneous tumor only was warmed and when the temperature reached 40°C, it was treated at 41-42°C for 40 min. Rectal temperature was monitored and controlled so that it did not exceed 38°C during HT.

**Tumor drug concentrations.** Two groups were established: group A in which 20 mg/kg of DXR-conjugate was administered intravenously (n=6), and group B which received 20 mg/kg of DXR-conjugate and HT (n=6). The dose of DXR-conjugate was determined as DXR equivalents. HT was completed in all animals within 1 h of the DXR-conjugate being administered and the mice were sacrificed 4 h (n=6 in each group) or 24 h (n=3 in each group) after the injection. The tumor was excised, weighed, and homogenized, 50% MeCN/0.5 N HCl was added to the homogenate, and then the mixture was centrifuged. The supernatant was collected and the concentrations of conjugated DXR and free DXR in the tumor were determined by high-performance liquid chromatography. The results were analyzed by Mann-Whitney U test, and statistically significant differences were identified.

**Antitumor efficacy.** Eight groups (n=6) were established: group I, no treatment; group II, DXR 10 mg/kg i.v.; group III, DXR-conjugate 10 mg/kg i.v.; group IV, DXR-conjugate 10 mg/kg i.v. + HT; group V, DXR 5 mg/kg i.v.; group VI, DXR-conjugate 5 mg/kg i.v.; group VII, DXR-conjugate 5 mg/kg i.v. + HT; and group VIII, HT. The experiment was started when the estimated weight of the tumors reached 200-400 mg. Tumor size was measured daily for 14 days after the treatments began. Mild HT at 41-42°C was induced for 40 min in groups A and B under the same conditions used for the experimental determination of the drug concentrations in the tumors. Because tumors implanted in nude mice do not usually exhibit sustained growth, antitumor efficacy was evaluated on the basis of relative growth. Estimated tumor volume at the start of the experiment was designated as  $V_0$ , and tumor volume on the day (n) of each determination ( $V_n$ ) was divided by  $V_0$  ( $V_n/V_0$ ). The mean  $V_n/V_0$  was calculated for each treatment group (VT) and in the control group (VC). The tumor inhibition rate (IR) was calculated as:  $IR = (1 - VT/VC) 100\%$  (21,22).

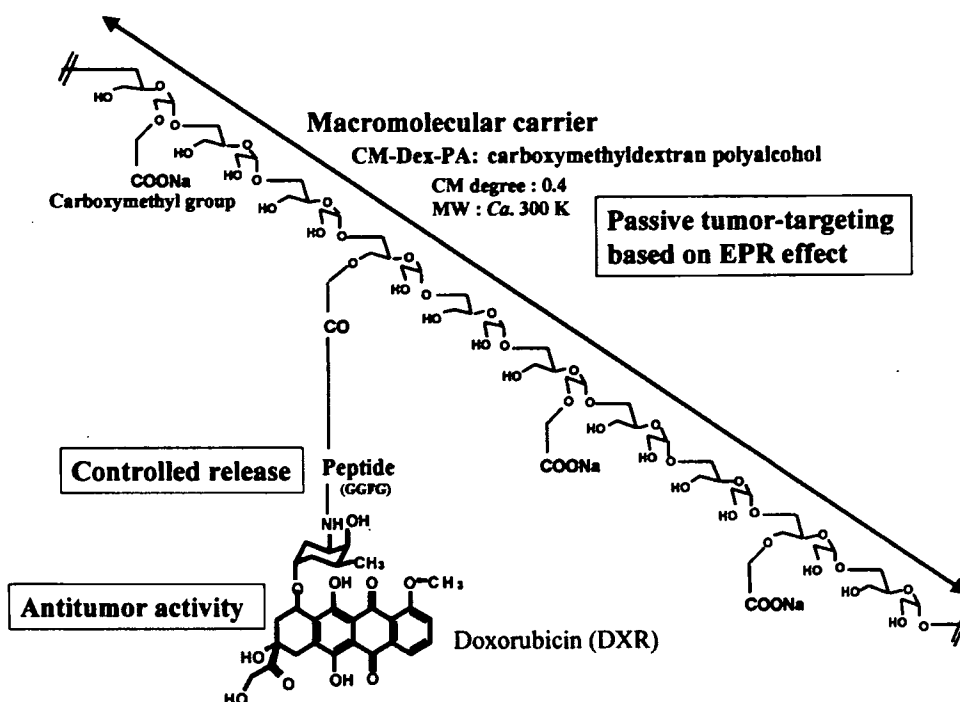


Figure 2. Partial structure of the doxorubicin (DXR)-conjugate (CM-Dex-PA-peptide-DXR).

Table I. Tumor concentrations of doxorubicin (DXR)-conjugate and free DXR at 4 h after administration with or without hyperthermia.

Group	Conjugated DXR ( $\mu\text{g/g}$ )	Free DXR ( $\mu\text{g/g}$ )	Total ( $\mu\text{g/g}$ )	Free/Total (%)
A (DXR-conjugate 20 mg/kg i.v.)	9.17 $\pm$ 1.18	0.56 $\pm$ 0.05	9.73 $\pm$ 1.16	6.23 $\pm$ 0.97
B (DXR-conjugate 20 mg/kg i.v. + HT)	19.04 $\pm$ 2.51 <sup>a</sup>	0.96 $\pm$ 0.17	20.00 $\pm$ 2.61 <sup>b</sup>	4.98 $\pm$ 0.78

<sup>a</sup>Statistically significant compared with conjugated DXR of group A.  $p=0.008$ . <sup>b</sup>Statistically significant compared with total of group A.  $p=0.007$ . Data are expressed as mean  $\pm$  SE.

Toxicity was determined by the decrease in body weight. The results were analyzed by Mann-Whitney U test, and statistically significant differences were identified.

## Results

**Tumor accumulation of DXR-conjugate with or without HT.** Table I shows the concentrations of conjugated DXR and free DXR in the excised tumors from group A (DXR-conjugate 20 mg/kg i.v.) and group B (DXR-conjugate 20 mg/kg i.v. + HT). The weight of the excised tumors was 541.07 $\pm$ 236.99 mg in group A and 550.72 $\pm$ 292.21 mg in group B, and the difference between the groups was not significant ( $p=0.379$ ). The mean concentration of conjugated DXR was 9.17 $\pm$ 1.18  $\mu\text{g/g}$  in group A and 19.04 $\pm$ 2.51  $\mu\text{g/g}$  in group B. Thus, the concentration of conjugated DXR was approximately doubled by combined use of HT, and the difference was significant ( $p=0.008$ ). The mean concentration of free DXR was

0.56 $\pm$ 0.05  $\mu\text{g/g}$  in group A and 0.96 $\pm$ 0.17  $\mu\text{g/g}$  in group B, and the difference was not significant ( $p=0.066$ ). The mean total concentration of conjugated DXR and free DXR was 9.73 $\pm$ 1.16  $\mu\text{g/g}$  in group A and 20.00 $\pm$ 2.61  $\mu\text{g/g}$  in group B, and thus the drug concentration in the tumor was approximately doubled by the combined use of HT, and the difference was significant ( $p=0.007$ ). The mean rate of DXR release calculated as the ratio of the concentration of free DXR to the total concentration (free DXR/total DXR) was 6.23 $\pm$ 0.97% in group A and 4.98 $\pm$ 0.78% in group B, and the difference between the groups was not significant ( $p=0.262$ ).

**Antitumor efficacy of DXR-conjugate with or without HT.** Because tumor blood flow volume is generally large when the growth rate is high, and decreases when the growth rate is low (23), the experiment was started at an appropriate time for assessing antitumor efficacy (i.e., when the estimated tumor weight reached  $\sim$ 300 mg). There were no significant



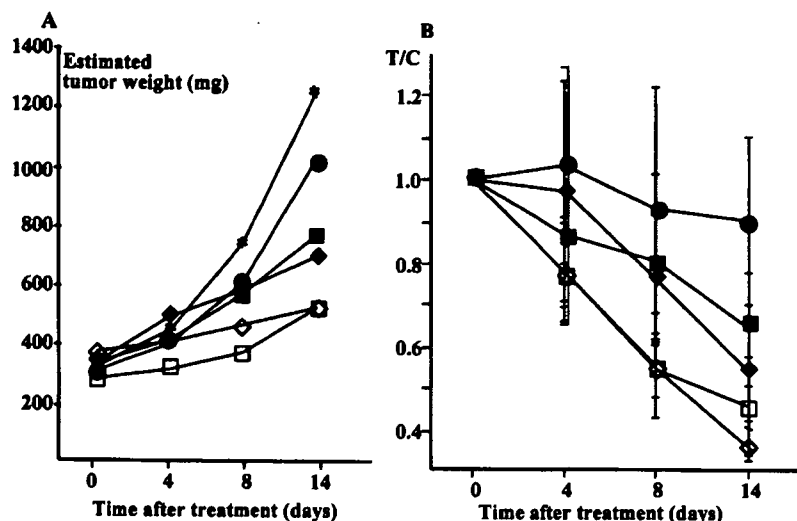


Figure 3. Individual tumor growth curves (A) and antitumor efficacy of doxorubicin (DXR)-conjugate with or without hyperthermia (HT) (B). \*, no treatment; ■, DXR-conjugate 5 mg/kg i.v.; ◆, 10 mg/kg i.v.; □, 5 mg/kg i.v. + HT; ◊, 10 mg/kg i.v. + HT; ○, HT.

Table II. Antitumor efficacy of doxorubicin (DXR)-conjugate with or without hyperthermia.

Group	Treatment	Estimated tumor weight (mg), mean $\pm$ SE	Relative tumor volume	Inhibition rate (%)
I	No treatment	1254.67 $\pm$ 163.3	1	0
II	DXR 10 mg/kg i.v.	989.3 $\pm$ 251.2	0.738	26.2 <sup>a</sup>
III	DXR-conjugate 10 mg/kg i.v.	701.9 $\pm$ 105.3	0.539	46.1 <sup>a,b</sup>
IV	DXR-conjugate 10 mg/kg i.v. + HT	527.4 $\pm$ 52.2	0.375	63.5 <sup>b</sup>
V	DXR 5 mg/kg i.v.	1175.6 $\pm$ 195.9	0.919	8.0 <sup>c</sup>
VI	DXR-conjugate 5 mg/kg i.v.	915.5 $\pm$ 189.1	0.638	36.2 <sup>c,d</sup>
VII	DXR-conjugate 5 mg/kg i.v. + HT	528.2 $\pm$ 106.5	0.479	52.0 <sup>d</sup>
VIII	HT	1032.8 $\pm$ 143.7	0.864	13.6

Estimated tumor volume (mg) = 0.5 x (length x width<sup>2</sup>). Relative tumor volume = (average tumor volume of each group)/(average tumor volume of group I). Inhibition rate (%) = (1 - relative tumor volume) x 100. <sup>a</sup>p=0.0492, <sup>b</sup>p=0.0039, <sup>c</sup>p=0.0104, <sup>d</sup>p=0.0250.

differences between any of the groups in estimated tumor weight at the start of the experiment. The growth rate of the implanted tumor increased after the estimated weight exceeded 300 mg, and the growth rate increased ~1.5-fold after the weight exceeded 400 mg (Fig. 3A). Tumor size in the control group increased ~4-fold within 14 days (Fig. 3A). In group II (DXR 10 mg/kg i.v.) and group V (DXR 5 mg/kg i.v.). The inhibition rate (IR), which reflects antitumor efficacy, was 26.2 and 8.0%, respectively, as opposed to 46.1 and 36.2% in group III (DXR-conjugate 10 mg/kg i.v.) and group IV (DXR-conjugate 5 mg/kg i.v.), respectively. Comparison of DXR-conjugate and DXR at the same doses revealed significant enhancement of drug activity in groups III and VI (p=0.0492, p=0.0104), demonstrating the usefulness of the DXR-conjugate as a DDS compound (Table II). IR was significantly increased by HT at every dose (Table II) and was cytotoxic in group VIII.

Kumazawa *et al* have shown that a DDS using the CM-Dex-PA carrier reduced toxicities (10) and Shiose *et al* reported that the DXR-conjugate has lower toxicities than DXR alone (personal communication). In the present study the side effects of DXR-conjugate with HT were evaluated on the basis of body weight loss (Fig. 4, Table III). Comparison of the weight loss in groups III and IV and groups VI and VII showed that the differences were not significant (p=0.1282, p=0.1093), but the weight loss in the groups with HT (IV and VII) tended to be less than in the groups without HT (III and VI). Group VIII (HT) lost the least body weight.

## Discussion

There is a long history of macromolecular drugs and a number of studies have been conducted since 1975 when the basic model was proposed by Ringsdorf (24). The DXR-conjugate

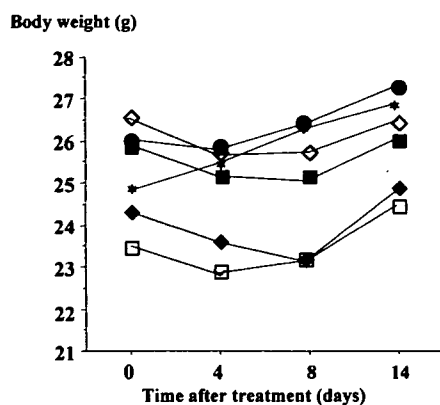


Figure 4. Change in body weight. \*, no treatment; ■, DXR-conjugate 5 mg/kg i.v.; ●, 10 mg/kg i.v.; □, 5 mg/kg i.v. + HT; ◇, 10 mg/kg i.v. + HT; ●, HT.

Table III. Toxicity of treatment with doxorubicin (DXR)-conjugate with or without hyperthermia.

	BWLmax % (day)
No treatment	0
DXR-conjugate (10) i.v.	4.9 (8)
DXR-conjugate (10) + HT	3.4 (4)
DXR-conjugate (5) i.v.	3.9 (8)
DXR-conjugate (5) + HT	3.2 (4)
HT	0.5 (4)

BWLmax, maximum rate of body weight loss.

Table IV. Tumor concentrations of doxorubicin (DXR)-conjugate and free-DXR 24 h after administration with or without hyperthermia.

	Conjugate DXR ( $\mu\text{g/g}$ )	Free DXR ( $\mu\text{g/g}$ )	Total ( $\mu\text{g/g}$ )	Free/Total (%)
DXR-conjugate 20 mg/kg i.v.	4.41 $\pm$ 1.55	4.02 $\pm$ 0.85	8.427 $\pm$ 2.38	50.20 $\pm$ 5.53
DXR-conjugate 20 mg/kg i.v. + HT	9.50 $\pm$ 2.06	6.28 $\pm$ 0.90	15.78 $\pm$ 2.97	40.57 $\pm$ 2.09

Data are expressed as mean  $\pm$  SE.

was developed from the concept that long-term high retention of the conjugate in the blood leads to an efficient EPR effect, and release of DXR in the tumor, but not in the blood (Shiose *et al*, personal communication). The DXR-conjugate also showed both biocompatibility (i.e., not recognized as a foreign body in the reticuloendothelial system and no antigenicity) and appropriate excretion, because of its hydrophilicity and the charge of the CM-Dex-PA [polyalcoholization (PA) and carboxymethylation (CM) of Dex] carrier. Because of its high mean molecular weight (approximately 300 kDa), the DXR-conjugate does not pass through the glomerular filter, and high concentrations are maintained in the blood. The anti-cancer effect of DXR is dose-dependent, and its rate of release is an important factor in its efficacy. The rate of release is controlled by the peptidyl spacer and varies with the combination of amino acids. Because a peptidyl spacer with a high release rate is considered appropriate for use with dose-dependent anticancer drugs such as DXR, we used GGFG (Gly-Gly-Phe-Gly) for the DXR-conjugate. The biotransformation of DXR-conjugate and DXR in MethA-cancer-bearing mice was shown by Shiiose *et al* (personal communication). The area under the blood concentration-time curve of DXR-conjugate in the tumor during the period from 2 to 48 h ( $\text{AUC}_{2-48\text{ h}}$ ) was approximately twice as high as that of DXR, and the  $\text{AUC}_{2-48\text{ h}}$  of DXR-conjugate in the liver was approximately 50% higher than that of DXR. The tumor selectivity of the DXR-conjugate (tumor  $\text{AUC}_{2-48\text{ h}}$ /liver  $\text{AUC}_{2-48\text{ h}}$ ) was approximately 4-fold higher than that of DXR.

*Tumor accumulation of DXR-conjugate with or without HT.* Cancer therapy based on the EPR effect of macromolecular and liposome preparations has attracted interest in the last decade (25-30), and research on treatment methods that combine administration of such preparations with HT is also progressing. Some studies have shown that tumor accumulation of macromolecular and liposome preparations is increased by HT-induced microenvironmental changes in tumor tissue (29,31-34). In general, mild HT at 39-42°C induces an increase in tumor tissue blood flow volume (15,16), tumor vessel hyperpermeability and extravasation (35-39). However, HT at 43°C or higher temperatures induces vascular injury, haemorrhage, and collapse, and a decrease in extravasation (38,40-43). Thus, the effect of HT on tumor tissue and tumor drug accumulation varies with the thermal dose. In the present study HT was conducted at 41-42°C for 40 min to increase tumor accumulation of DXR-conjugate. The drug's concentration in the tumors was determined 4 h after administration (i.e., when the change in tumor tissue induced by HT was most prominent). After the combination treatment, the concentration of conjugated DXR and the total drug concentration (conjugated DXR + free DXR) in the tumor was approximately doubled. At 4 h after administration there was no significant difference in the rate of DXR release (free DXR/total dose) between administration with and without HT, suggesting that the rate of drug release is unaffected by HT. The drug's concentration in the tumors was determined 24 h after administration to investigate differences in drug concentrations in the tumor. Both the

concentration of conjugated DXR and total dose of drugs were less than at 4 h after administration in both the DXR-conjugate group and DXR-conjugate + HT group. However, the total dose of drugs was still approximately 2-fold higher than baseline at 24 h after administration, and the drug concentration in the tumor was still higher when HT was used (Table IV). These results support the suggestion that HT has an effect on the pharmacokinetics of DXR-conjugate, and the results were similar to those of conventional studies in which HT has been combined with liposomes (31,44). The widening and opening of gaps between endothelial cells may account for the increased tumor drug delivery (31,36,38,39,45). Functional and structural studies have shown that large pores exist in tumor vessels (46). Hyperthermic conditions lead to a rapid reduction and rearrangement of endothelial cell F-actin stress fibres (47,48), which would allow larger pores to be formed between cells (39). If the HT does not exceed 43°C, the change in the endothelium appears to be reversible within 24 h (47). One study in a model of ovarian carcinoma (SKOV-3) showed that 6 h after HT (41°C for 1 h) the degree of extravasation of nanoparticles had returned to baseline (38). Thus the tumor model used, the size of the drug, and the thermal dose affect the results.

*Antitumor efficacy of DXR-conjugate with or without HT.* From the findings of the dose-response relationship after administering 1.25-30 mg/kg of DXR-conjugate (data not shown), the maximum tolerated dose (MTD) of DXR-conjugate in nude mice was estimated to be approximately 40 mg/kg, and one-quarter and one-eighth of the MTD were used in the assessment of antitumor efficacy. The IR increased from 26.2 to 46.1% in the DXR 10 mg/kg group and DXR-conjugate 10 mg/kg group and from 8.0 to 36.2% ( $p < 0.05$ ) in the DXR 5 mg/kg group and the DXR-conjugate 5 mg/kg group respectively. Tashiro reported that the MTD of DXR in nude mice is 12 mg/kg, with an IR of LU99 cells of 28% (22). In the present study the IR of DXR 10 mg/kg was nearly equal to that of DXR at the MTD. Another study has shown that the sensitivity of LU99 to DXR is probably low because of the distribution of DXR in the tumor tissue, which depends on the pH (49,50) and is higher in the range of 6.2-7.6 (50). The results of the present study show that antitumor efficacy was enhanced by using a DDS with a macromolecular carrier (i.e., accumulation of DXR in tumor tissue).

Comparison of the IR in the DXR-conjugate 10 mg/kg group and the DXR-conjugate 10 mg/kg i.v. + HT group showed that it increased from 46.1 to 63.5%, and from 36.2 to 52.0% ( $p < 0.05$ ) between the DXR-conjugate 5 mg/kg and DXR-conjugate 5 mg/kg + HT groups. Thus, antitumor efficacy was enhanced to almost the same extent, 16-17 points, in the groups in which HT was used. Because the IR was 13.6% in the group treated with HT alone, we consider that enhancement of the antitumor efficacy of the DXR-conjugate by HT is an additive effect to its own cytotoxic effect of HT (Tables III and IV). The evaluation of the toxicity of DXR-conjugate using weight loss as an indicator showed that toxicity tended to be reduced by the combined use of HT. The specific mechanism remains unknown, but one possible reason is that the drug's concentration in the tumor

was enhanced and thus the tumor selectivity of the DXR-conjugate was increased by the combined use of HT.

A newly synthesized compound, DXR-conjugate, exerted antitumor efficacy that was significantly superior to that of DXR alone in a nude mouse model. In addition, combined use of DXR-conjugate and HT resulted in an increase in the DXR-conjugate concentration in the tumor, significantly enhancing the drug's antitumor efficacy. Using weight loss as an indicator, toxicity was not increased by the combined use of HT.

## References

- Lowenthal RM and Eaton K: Toxicity of chemotherapy. *Hematol Oncol Clin North Am* 10: 967-990, 1996.
- Matsumura Y and Maeda H: A new concept for macromolecular therapeutic in cancer chemotherapy: mechanism of tumor-tropic accumulation of proteins and antitumor agent smancs. *Cancer Res* 46: 6387-6392, 1975.
- Maeda H, Wu J, Sawa T, Matsumura Y and Hori K: Tumor vascular permeability and EPR effect in macromolecular therapeutics: a review. *J Control Release* 65: 271-284, 2000.
- Maeda H: The enhanced permeability and retention (EPR) effect in tumor vascular: the key role of tumor-selective macromolecular drug targeting. *Adv Enzyme Regul* 41: 189-207, 2001.
- Dvorak H: Identification and characterization of the blood vessels of solid tumors that are leaky to circulating macromolecules. *Am J Pathol* 133: 95-109, 1998.
- Jain R: Extravascular transport in normal and tumor tissue. *Crit Rev Oncol Hematol* 5: 115-170, 1986.
- Inoue K: Glyco-technology and DDS. *Farumashia* 29: 1256-1260, 1993.
- Nogusa H: Synthesis of carboxymethylpullulan-peptide-doxorubicin conjugates and their properties. *Chem Pharm Bull* 43: 1931-1938, 1995.
- Sugawara S: Characteristics of tissue distribution of various polysaccharides as drug carriers: influences of molecular weight and anionic charge on tumor targeting. *Biol Pharm Bull* 24: 535-543, 2001.
- Kumazawa E and Ochi Y: DE-310, a novel macromolecular carrier system for the camptothecin analog DX-8951f: potent antitumor activities in various murine tumor models. *Cancer Sci* 95: 168-175, 2004.
- Masubuchi N: Pharmacokinetics of DE-310, a novel macromolecular carrier system for the camptothecin analog DX-8951f, in tumor-bearing mice. *Pharmazie* 59: 374-377, 2004.
- Engin K: Thermoradiotherapy in the management of superficial malignant tumors. *Clin Cancer Res* 1: 1139-1145, 1995.
- Field SB: An Introduction to the Practical Aspects of Clinical Hyperthermia. Taylor and Francis: London, 1990.
- Dewhirst M, Prosnitz L, Tharll D. *et al*: Hyperthermic treatment of malignant diseases: current status and a view toward the future. *Semin Oncol* 24: 616-625, 1997.
- Karino T, Koga S and Maeta M: Experimental studies of the effects of local hyperthermia on blood flow, oxygen pressure and pH in tumors. *Jpn J Surg* 18: 276-283, 1988.
- Song CW: Effect of local hyperthermia on blood flow and micro-environment (Review). *Cancer Res* 44 (suppl 1): S4721-S4730, 1984.
- Engin K: Biological rationale and clinical experience with hyperthermia. *Control Clin Trials* 17: 316-342, 1996.
- Feyerabend T: Rationale and clinical status of local hyperthermia, radiation and chemotherapy in locally advanced malignancies. *Anticancer Res* 17: 2895-2897, 1997.
- Issels R: Hyperthermia combined with chemotherapy: biological rationale, clinical application and treatment results. *Oncology* 22: 374-381, 1999.
- Matthew CB: Hyperthermia-induced changes in the vascular permeability of rats: a model system to examine therapeutic interventions. *J Thermal Biol* 25: 381-386, 2000.
- Inaba M: Evaluation of antitumor activity in a human breast tumor/nude mouse model with a special emphasis on treatment dose. *Cancer* 64: 1577-1582, 1989.
- Tashiro T: Responsiveness of human lung cancer/nude mouse to antitumor agents in a model using clinically equivalent doses. *Cancer Chemother Pharmacol* 24: 187-192, 1989.